

# Annealing of Nanometer-Sized Zinc Oxide Particles

Volker Noack and Alexander Eychmüller\*

*Institute of Physical Chemistry, University of Hamburg, Bundesstrasse 45,  
20146 Hamburg, Germany*

*Received October 25, 2001. Revised Manuscript Received November 28, 2001*

The processes occurring during annealing of particulate ZnO thin films and powders are examined in detail by size-determining methods (TEM and powder X-ray diffraction) and by thermal analysis. Water and carbon dioxide desorb from the surface at temperatures of about 100 °C. At higher temperatures (between 300 and 500 °C), two processes are observed: a change in the chemical composition of the surface by thermal degradation of adsorbed molecules and an increase of the geometric particle size. A structural model for nanometer-sized ZnO nanocrystals is proposed according to which the core of the particles consists mainly of pure ZnO surrounded by a shell containing Li<sup>+</sup> and ZnO. Acetate ions adsorbed on this shell form the outermost layer. To account for the low energy shift in the absorption spectra of the larger particles, an interaction of the adsorbed acetate ions with the electrons inside the ZnO is suggested which contributes to the observed size-quantization of the tiny semiconductors.

## Introduction

Semiconducting metal oxides have gained major importance in catalysis and electrooptical research. Especially, polycrystalline thin film electrodes of TiO<sub>2</sub>, ZnO, and SnO<sub>2</sub> are of considerable interest for current applications in photovoltaics and electrooptical devices. Such films possess a large internal surface which is accessible for further modifications thus strongly motivating their use as substrates in this field. Although the substrates themselves are of minor interest in most cases, some of their basic properties must be well understood. For that, many publications deal with the characterization of such polycrystalline samples. In particular, it is possible to obtain thin films using a large variety of different techniques such as sputtering,<sup>1</sup> spray pyrolysis,<sup>2</sup> or chemical vapor deposition.<sup>3</sup> These samples tend to show strongly varying properties which are sensitively dependent on the conditions of the employed method. On the contrary, wet chemical synthetic routes offer an easy way to yield colloidal solutions with a large range of particle sizes on the gram-scale in combination with high reproducibility.

For this chemical approach, a lot of work has been done on the preparation of nanometer-sized semiconductor particles in solution and in thin films. If the sizes of these crystallites are on the order of the Bohr radius of their exciton, the electronic band gap shows a strong increase indicating the additional kinetic energy of the exciton due to its spatial confinement, the so-called size-quantization.<sup>4</sup> This effect allows a fine-tuning of the

positions of the electronic bands in an experimentally accessible size range. In the past two decades, most of the investigations of this effect have been done on metal sulfides, selenides, and phosphides.<sup>5</sup> Since the Bohr radius of most of the metal oxides is very small (about 1 nm), only a few oxides show this size-quantization. One of these few materials is ZnO<sup>6</sup> which is of high interest for many technical applications: e.g., in varistors,<sup>7</sup> photovoltaic cells,<sup>8–10</sup> and as transparent conducting films.<sup>11</sup> With the use of the sol–gel technique, colloidal solutions of ZnO can be gained by different preparative methods,<sup>12–14</sup> and their growth kinetics as well as their optical and electronic properties have been the subject of detailed investigations.<sup>13–16</sup> Though permitting control of the particle size and surface during the wet chemical synthesis, for future applications it would be most desirable to employ a post-preparative treatment of nanoparticulate samples to adjust their specific properties as it is most common for the fabrication of “dense” ZnO films.<sup>1,17,18</sup>

(5) For a comprehensive review, see, e.g., Eychmüller, A. *J. Phys. Chem. B* **2000**, *104*, 6514 and references therein.

(6) Koch, U.; Fojtik, A.; Weller, H.; Henglein, A. *Chem. Phys. Lett.* **1985**, *122*, 507.

(7) Gupta, T. K. *J. Am. Ceram. Soc.* **1990**, *73*, 1817.

(8) Tennakone, K.; Senadeera, G. K. R.; Perera, V. P. S.; Kottegoda, I. R. M.; De Silva, L. A. A. *Chem. Mater.* **1999**, *11*, 2474.

(9) Rensmo, H.; Keis, K.; Lindström, H.; Södergren, S.; Solbrand, A.; Hagfeldt, A.; Lindquist, S.-E.; Wang, L. N.; Muhammed, M. *J. Phys. Chem. B* **1997**, *101*, 2598.

(10) Vogel, R.; Hoyer, P.; Weller, H. *J. Phys. Chem.* **1994**, *98*, 3183.

(11) Hilgendorff, M.; Spanhel, L.; Rothenhäusler, C.; Müller, G. *J. Electrochem. Soc.* **1998**, *145*, 3633.

(12) Zou, B. S.; Volkov, V. V.; Wang, Z. L. *Chem. Mater.* **1999**, *11*, 3037.

(13) Spanhel, L.; Anderson, M. A. *J. Am. Chem. Soc.* **1991**, *113*, 2826.

(14) Bahnemann, D. W.; Kormann, C.; Hoffmann, M. R. *J. Phys. Chem.* **1987**, *91*, 3789.

(15) Meulenkamp, E. A. *J. Phys. Chem. B* **1998**, *102*, 5566.

(16) Wong, E. M.; Bonevich, J. E.; Searson, P. C. *J. Phys. Chem. B* **1998**, *102*, 7770.

\* To whom correspondence should be addressed. Email: eychmuel@chemie.uni-hamburg.de.

(1) Gupta, V.; Mansingh, A. *J. Appl. Phys.* **1996**, *80* (2), 1063.

(2) Ma, T. Y.; Moon, H. Y. *J. Mater. Sci.: Mater. Electron.* **1998**, *9*, 435.

(3) Tran, N. H.; Hartmann, A. J.; Lamb, R. N. *J. Phys. Chem. B* **1999**, *103*, 4264.

(4) Alivisatos, P. *Science* **1996**, *271*, 933.

The aim of the present study is to improve the preparation of particulate ZnO powders and thin films by using a post-preparative approach and provide more structural information about this system to facilitate applications as substrates in the science of materials.

### Experimental Section

**Preparation of the ZnO Particles.** Colloidal solutions of ZnO particles (2 nm in diameter) were obtained according to the method described by Spanhel and Anderson.<sup>13</sup> Briefly, a turbid suspension of 11.0 g of zinc acetate dihydrate (98+ %, Aldrich) in 500 mL of ethanol (p. a., Merck) was heated until the solution became clear. After this solution was refluxed for 1 h, 300 mL of the solvent was removed by distillation and replaced by the same amount of fresh ethanol. To the cooled (0 °C) suspension, 2.9 g of lithium hydroxide monohydrate (p. a., Fluka) was added in an ultrasonic bath to obtain a transparent solution consisting of small ZnO particles with diameters of about 2 nm. This solution was filtered through a 0.1  $\mu\text{m}$  glass fiber filter to remove undissolved LiOH.

To achieve particles with a diameter of 6 nm, a method developed by Hoyer and co-workers was used.<sup>19</sup> The solution containing the 2 nm particles was heated and mixed with a small amount of deionized water at 60 °C. During this procedure, the particles agglomerated and precipitated. The colorless precipitate was separated from the supernatant solution by centrifugation. Afterward, the precipitate was washed with an ethanol–water mixture (95:5) and centrifuged again. The last two steps were repeated four times to ensure the removal of physisorbed ionic compounds.

**Preparation of the ZnO Films.** To prepare thin films of the ZnO nanoparticles, the washed precipitate was diluted with a few milliliters of ethanol. For future electrochemical investigations, the resulting viscous suspension was spin-coated onto ITO substrates using a home-built apparatus. Residual solvent was evaporated by heating the samples in a furnace at 100 °C. To obtain thicker films, the coating procedure was repeated several times. The final film thickness was found to strongly depend on the viscosity of the colloidal suspension. Finally, the films were annealed for 30 min at temperatures between 100 and 500 °C.

For powder X-ray diffraction (XRD) measurements, the washed precipitate was ground in an agate mortar and dispersed in ethanol to achieve a better spreading on the silicon sample holder. The diffractometer (X<sup>PERT</sup>, Philips; wavelength, Cu K $\alpha$  = 154.1 pm) was equipped with a heatable holder (PW3020; heating rate, 25 °C/min). For comparison with the ex situ annealed ZnO, some samples were prepared by raking the viscous suspension onto a glass substrate followed by annealing at the desired temperature (100–500 °C). After being cooled to room temperature, the ZnO was scraped off with a scalpel. The corresponding diffractograms were recorded at room temperature.

Transmission electron microscope (TEM) images of the particulate samples were obtained by using a CM 300UT microscope (Philips; acceleration voltage, 300 kV) in combination with a CCD camera (Gatan 694). The particulate film was scraped off from the ITO substrate and dispersed in a few milliliters of ethanol in an ultrasonic bath. A droplet of this dispersion was placed on a copper grid which was first covered with a carbon film. The excess solution was subsequently removed by using a paper tip.

For a C/H/Li analysis, a sample consisting of smaller particles was used to achieve a larger surface area and thus facilitate the detection of adsorbed substances. For that purpose, the 2 nm sized colloid was mixed with a small amount

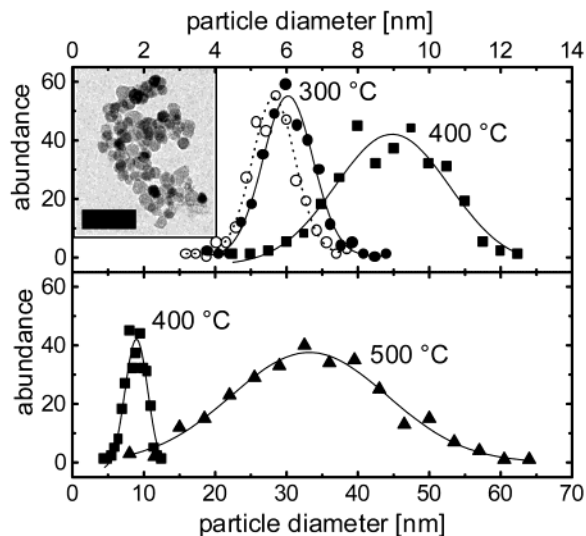


**Figure 1.** Size distribution of a particulate ZnO film as prepared (dotted line and open circles) and annealed at different temperatures (solid lines and solid symbols) as determined from TEM images. As an optical guideline, the corresponding fitted data assuming a Gaussian distribution are shown as lines in this diagram. (For better comparison, the distributions are presented on different size scales with the data of the sample annealed at 400 °C appearing in both parts of the diagram.) The inset in the upper part shows a transmission electron image representative for the not annealed sample (the bar corresponds to a length of 40 nm).

of water at room temperature. The resulting precipitate was thoroughly washed 10 times and dried in an oil pump vacuum. The analysis was carried out in the microanalytic laboratory Pascher in Remagen, Germany.

A thermogravimetric analysis of the annealing process in the temperature range between 30 and 800 °C was performed using a simultaneous thermal analyzing system (STA 409/C MS, Netzsch; heating rate, 5 °C/min) in combination with a mass spectroscopic detection unit (QMG 421, Balzer). For detection, it was necessary to specify the expected ratios of mass  $m$  to charge  $z$  prior to the data acquisition. The ratios of  $m/z$  chosen to be observed were 1, 2, 14, 15, 16, 17, 18, 27, 28, 29, 31, 32, 40, 44, 45, 59, 60, and 88.

Absorption measurements of the particulate ZnO films were performed by using an UV–vis spectrophotometer (lambda 40, Perkin-Elmer) with no sample in the reference beam.

### Results

A transmission electron micrograph of the scraped-off ZnO thin film prior to the annealing is shown in the inset in the upper part of Figure 1. The ZnO particles have mainly the same size and possess a spherical shape. A major change in size or shape of the nanocrystals did not occur in samples annealed at temperatures below 300 °C. At higher annealing temperatures, a growth of the nanocrystals was observed in the micrographs. For a sample annealed at 500 °C, the particles became irregular in shape, some of them became even clearly hexagonal.

By evaluating the sizes of a statistically significant number of particles (about 300 per sample), size distributions were obtained. For samples annealed at different temperatures, the resulting distributions are depicted in the upper and lower parts of Figure 1. Up to an annealing temperature of 300 °C, there was no significant change in the particle size as well as in the

(17) Kamalasanan, M. N.; Chandra, S. *Thin Solid Films* **1996**, *288*, 112.

(18) Bekmann, H. H. P. Th.; Benoist, K. W.; Joppe, J. L. *Appl. Surf. Sci.* **1993**, *70–71*, 347.

(19) Hoyer, P.; Eichberger, R.; Weller, H. *Ber. Bunsen-Ges. Phys. Chem.* **1993**, *97*, 630.

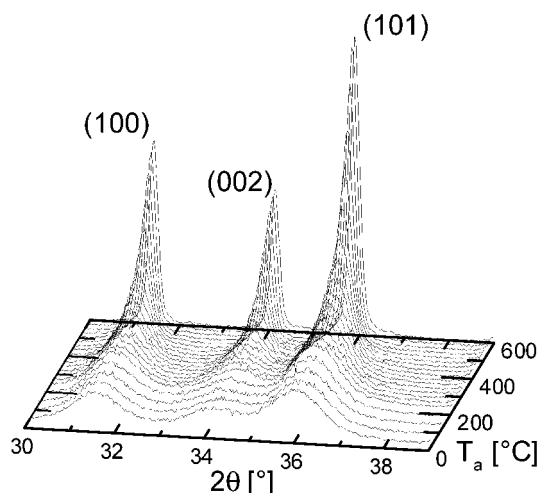


**Figure 2.** Evolution of the three most intense peaks in a powder X-ray diffractogram of a particulate ZnO sample during in situ annealing of the nanoparticles.

size distribution. For temperatures above 400 °C, the mean particle diameter increased with increasing annealing temperature accompanied by a strong broadening of the size distribution.

The X-ray diffractograms of all in situ annealed samples measured in a range between 5 and 70° are in good agreement with the available data of macroscopic hexagonal zincite<sup>20</sup> with respect to the position and relative intensity of the peaks. The particles exhibit good crystallinity with no indication for the existence of amorphous domains in the sample. In the temperature interval between 30 and 600 °C, no phase transition was observed. Furthermore, no peaks corresponding to other crystalline material being present in the sample (e.g., Li<sup>+</sup> or Zn<sup>2+</sup> salts) were found in the diffractograms. In Figure 2, for the three most intense peaks, the apparent changes in the diffractograms of a particulate ZnO powder during an in situ annealing are shown. At temperatures below 300 °C, no influence of the annealing temperature was observed on the peaks each having a low intensity and a broad peak shape. At temperatures above 300 °C, the width of the peaks decreases in association with a strong increase of their intensities. This observation can be explained by the theory of Scherrer which relates the full width  $\beta$  of a peak at half-maximum to the extension  $d$  of the crystalline domains in a polycrystalline sample according to  $d = 57.3\lambda K / (\beta \cos \theta)$ .<sup>21</sup> In this formula,  $\lambda$  denotes the X-ray wavelength,  $\theta$  is the Bragg angle, and  $K$  is a constant depending on the geometry of the crystallites (for an assumed spherical shape,  $K$  has to be unity<sup>22</sup>). With the use of this relation, diameters of the crystalline domains (i.e., of the particles) are obtained which indicate that the growth is slightly more prominent in the crystallographic  $c$ -axis (ranging from 6.6 to 52.0 nm for the (002) peak) than in the other directions (ranging from 7.2 to 48.2 nm for the (100) peak as well for the (101) peak).

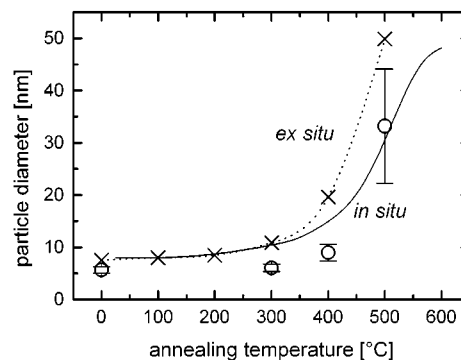


**Figure 3.** Mean particle diameter after annealing at different temperatures as determined by TEM (circles) and XRD (solid line, ZnO sample annealed in situ; dotted line/crosses, sample annealed prior to XRD experiments). The error bars shown reflect the standard deviation as determined from a fitted Gaussian distribution function (TEM data, cf. Figure 1).

For the in situ annealed ZnO sample, the mean value of the three crystallite sizes (in (100), (101), and (002) directions) is shown in Figure 3 as a function of the annealing temperature (solid line). For comparison, the particle sizes obtained from the TEM images are also presented in this diagram (circles). All samples show a strong increase of the particle size for annealing temperatures higher than 300 °C. The ZnO nanocrystals annealed in situ (solid line) exhibit a less pronounced growth in this temperature range than the particles annealed prior to the measurements (dotted line/crosses). As seen from additional XRD experiments (not shown here), it is the temperature rather than the duration of the annealing which determines the particle size.

Furthermore, the particle size of the latter sample as determined by the Scherrer method is clearly bigger than the size resulting from the TEM evaluation (circles). As indicated by the decreasing slope at temperatures above 600 °C, the in situ annealed particles seem to reach a maximum size of about 50 nm.

As a consequence of the wet chemical synthesis, lithium ions as well as organic molecules (acetic acid, acetate, and ethanol) may be present in the particulate ZnO sample. To determine the total amount of these substances, an elemental analysis of the nanocrystals was performed. According to this analysis, the relative masses obtained were C/H/Li of 4.45:0.55:2.88 wt % (corresponding to a molar ratio of 1.0:1.49:1.11). The molar ratio of C/H is thus quite low being close to the ratio of 1:1.5 of the acetate anion.

Additionally, a detailed thermal analysis was carried out. In the upper part of Figure 4, the mass loss of as-prepared ZnO particles is shown. In the temperature range between 50 and 130 °C, a relative loss of 4.8 wt % has been observed, followed by a loss of only 1.5 wt % at temperatures between 130 and 260 °C, and finally a loss of 6.9 wt % at about 350 °C, no matter whether the experiments were carried out under argon or in air. A ZnO sample which was annealed at 500 °C prior to the thermal analysis showed a mass loss of less than 0.2 wt % in the same temperature interval.

For a better understanding of the processes occurring at the surface of the particles during the annealing process, the molecules being released from the sample by desorption or decomposition at elevated temperatures

(20) Powder diffraction file No. 36-1451.

(21) Kruschner, H. *Einführung in die Röntgenfeinstrukturanaalyse*; Friedr. Vieweg & Sohn: Braunschweig, 1993.

(22) Wilson, J. C. *Röntgenstrahl-Pulverdiffraktometrie: Mathematische Theorie*; Philips: Hamburg, 1965.



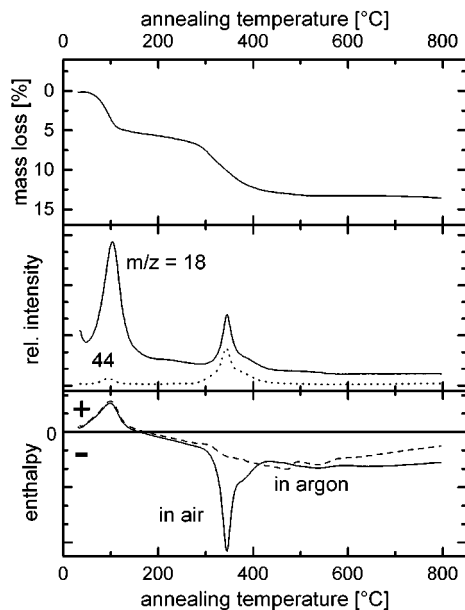


**Figure 4.** Thermal analysis of a particulate ZnO sample: upper part, thermogravimetric mass loss during annealing in air of an as-prepared ZnO sample; middle part, relative mass spectroscopic abundance of fragments with a  $m/z$  ratio of 18 and 44 (corresponding to water and carbon dioxide being released during the annealing); lower part, differential scanning calorimetry of as-prepared ZnO nanoparticles, performed under argon and in air.

were analyzed using a mass spectroscopic detection. In the middle part of Figure 4, the relative abundance of fragments with a ratio of  $m/z$  being 18 and 44 are shown as a function of the annealing temperature. Thus, at about 100 °C, water ( $m/z = 18$ ; solid line) and carbon dioxide (or acetaldehyde, both having  $m/z = 44$ ; dotted line) are desorbed from the surface. At temperatures between 300 and 400 °C, the release of water and carbon dioxide is observed, the latter having a higher abundance at these temperatures than at low temperatures. These fragments are ascribed to the thermal decomposition of adsorbed acetate or acetic acid.

Other observed fragments originate from oxygen ( $O^+$  ( $m/z = 16$ ) and  $O_2^+$  (32); detectable only for the measurement under argon), water ( $H_2^+$  (2) and  $OH^+$  (17)), and acetic acid ( $CH_3^+$  (15),  $CH_3COO^+$  (59), and  $CH_3COOH^+$  (60)). To a smaller extent, fragments corresponding to ethanol ( $CH_3CH_2O^+$  (45) and  $CH_3CH_2OH^+$  (46)) were found in the mass spectroscopic analysis. The abundance of this alcohol was at least 3 orders of magnitude smaller than that of acetic acid. The ethanol content of the powder is thus most likely due to traces of the residual solvent still present in the powder. The abundance of fragments with the following  $m/z$  ratio were not observed in the experiments: 14 (corresponding to  $CH_2^+$ ), 28 ( $C_2H_4^+$  or  $CO^+$ ), 31 ( $CH_3O^+$ ), 40 ( $C_3H_4^+$ ), and 88 ( $CH_3COOCH_2CH_3^+$ ).

With the thermal analysis performed under an inert argon atmosphere, the intensities of the mass spectroscopic signals of all fragments observed (except for  $m/z = 18$ ,  $H_2O^+$ ) were much lower than those for the experiments in air but were similar in their patterns of occurrence.

The lower part of Figure 4, presents the data received by differential scanning calorimetry of the ZnO nanoparticles. The process responsible for the mass loss at

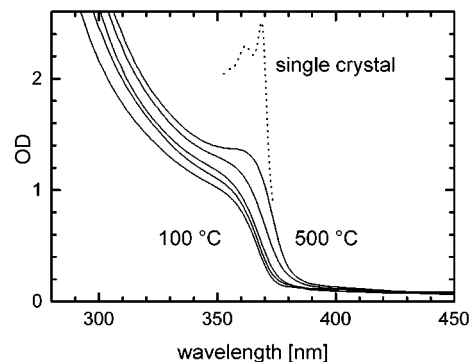


**Figure 5.** Absorption spectra of particulate ZnO thin films on ITO substrates. The samples have a thickness of about 250 nm and were annealed at different temperatures (from left to right: 100, 200, 300, 400, and 500 °C). Additionally, the spectrum of a macroscopic ZnO single crystal of a thickness of 100 nm is shown in a magnification of 2.5 (taken from ref 23).

100 °C is identified to be endothermic, while the loss at 350 °C is exothermic. Though the total amount of the loss is the same for samples annealed under argon and in air, the exothermic character of the latter is much more pronounced than that of the first one. This finding indicates that in the presence of oxygen, the predominant process is most likely an oxidation of the acetate, while in the absence of oxygen, a reductive decomposition is favored which is less exothermic.

In Figure 5, the absorption spectra of ZnO films are shown. These films had a thickness of approximately 250 nm and were annealed on the ITO substrates at different temperatures. As a reference, the spectrum of a ZnO single crystal is depicted (taken from ref 23). Since the data shown in ref 23 were obtained for a crystal of about 100 nm thickness, for a better comparison, this spectrum was multiplied by a factor of 2.5 to correspond to the thickness of the particulate films. However, the optical density of the nanocrystalline film is only 60% of the optical density of the macroscopic sample. The observed difference might reflect the porous structure of the particulate film rather than a size-dependent absorption coefficient of the ZnO crystallites. Thus, the volume occupied by the particles might be only 60% of the corresponding dense semiconductor which shows a good agreement with the value of 64% for the case of a random dense packing of spheres.<sup>24</sup>

With respect to their spectral positions, the absorption edge of the sample annealed at 500 °C corresponds very well with the absorption edge of the single crystal. The other samples show a distinct blue shift of the absorption edge which is more pronounced with lower annealing temperature.

## Discussion

The annealing process of particulate ZnO films can be divided into two major processes resulting in different changes of the sample: The first process is found at a temperature of about 100 °C. According to the differential thermal analysis, this is a slightly endothermic process which is most likely a reversible thermal de-

(23) Liang, W. Y.; Yoffe, A. D. *Phys. Rev. Lett.* **1968**, *20*, 59.

(24) Hench, L. L.; West, J. K. *Chem. Rev.* **1990**, *90*, 33.

sorption of water and carbon dioxide from the surface of the particles. Since both substances are present in the atmosphere, they might have been adsorbed from the ambient air during the storage of the thin films. At these temperatures, no major change of the geometric or electronic particle size is observed for the particulate samples.

The second process is observed after an annealing at temperatures between 300 and 450 °C. Under these conditions, the mass loss of the ZnO sample is dominated by a decomposition of acetate anions or acetic acid at the surface of the ZnO particles. This process is associated with an increase of the particle size, the magnitude of which depends on the annealing temperature. A similar temperature of 450 °C was observed to be necessary by Kamalasanan and Chandra for the conversion of an amorphous precursor into a conductive ZnO film using a sol-gel approach.<sup>17</sup>

The occurrence of this growth differs significantly from earlier studies on the same system by Hoyer and co-workers, in which no increase of the particle size was observed up to an annealing temperature of 500 °C.<sup>19</sup> These authors emphasized the role of Li<sup>+</sup> as a destabilizing component for a thermal treatment. Thus, the differences might arise from different Li<sup>+</sup> contents in the particles used by Hoyer et al. and those used in our work despite the similar preparation and washing procedures.

The growth process was monitored using TEM and XRD. The mean particle size as determined from the XRD data of in situ annealed ZnO was found to be smaller than the diameters of the samples annealed prior to the measurement. This finding may be attributed to the different annealing conditions: In the first case, the crystallites are heated slowly (at a rate of 5 °C/min). The nanocrystalline sample used for the second measurement was placed in the hot furnace resulting in a very fast increase of the temperature inside the sample and thus a strong deviation from equilibrium. It is feasible to assume that the latter conditions most probably result in a stronger growth of the nanocrystallites than the treatment under moderate conditions.

Additionally, the average diameter as determined by evaluation of the XRD measurement tends to be bigger than the corresponding data from TEM analysis. The Scherrer method delivers only estimates for the actual particle size, since in real systems, the surface and the measurement apparatus also contribute to the broadening of the peaks resulting in an estimation of the actual diameter. Thus, the finding of larger particles in the XRD measurements than in the TEM images is surprising. The difference may be explained by a pronounced lumping of ZnO particles annealed at high temperatures. Since the resulting lumps are not properly shown in the TEM images, they are not sufficiently considered in the size histograms and thus the size-distribution function itself would be displaced toward smaller diameters. On the other hand, the broadening of the XRD peaks takes into account the sizes of all crystallites. Despite its lack in applicability to small (irregular) particles, the Scherrer method might be more suitable for the determination of the average particle sizes of large ZnO particles than TEM images. Furthermore,

with the particle sizes being smaller, as determined from the TEM images than by XRD measurements, they give rise to the conclusion that a particle consists mainly of pure ZnO (i.e., without having a surrounding shell of other solid material). This finding is supported by the lack of additional XRD patterns corresponding to other crystalline materials in the sample.

The apparent plateau pretending a maximum particle size of about 50 nm might be attributed to different causes: First, this observation may be due to the existence of a real maximum size which might limit a growth process for geometric reasons. A further increase of the size might be possible only in a coherent recrystallization process requiring even higher temperatures. On the other hand, the applicability of the Scherrer formula is restricted to small particles (smaller than 100 nm).<sup>25</sup> Thus, the existence of a maximum size might reflect the restriction of the validity of the Scherrer formula for the growing ZnO crystallites. In this case, the width of the XRD peaks for samples annealed at temperatures above 550 °C might be only due to contributions of the apparatus.

From the XRD patterns of the ZnO, it was excluded that the sample contains other crystalline or amorphous substances. Therefore, the growth observed during the annealing cannot be a simple epitaxial crystallization process of amorphous ZnO or of a precursor left over after the wet chemical synthesis. It should rather be a thermally assisted fusing of adjacent crystallites or a competitive growth process, in which the number of smaller particles is reduced in favor of the growth of bigger ones. The first process is proposed by Spanhel and Anderson for ZnO particles in solution during an early stage of their growth.<sup>13</sup> This process should not be associated with the observed particle sizes changing continuously during annealing but rather with a growth in distinct multiples of the initial particle size. For that reason, preferably, a competitive growth has to be assumed as is described by the well-known model for a reduction in the surface free energy according to Ostwald. For the description of the growth in colloidal solutions corresponding to the Ostwald ripening, usually the treatment of Lifshitz, Slyozov,<sup>26</sup> and Wagner<sup>27</sup> ("LWS" theory) is chosen which results in a skewed distribution function of the particle sizes during the growth.<sup>16</sup> As can be seen from Figure 1, such a behavior is not observed in the present case of ZnO particles. An explanation could be that the LWS theory describes a competitive growth of colloids having a big interparticle distance (and thus a low volume fraction) and is limited only to a mass transport through the dispersing medium, the solvent. Since both of these assumptions do not hold for the annealing of a particulate powder, the difference between the LWS model and the growth mechanism of the ZnO particles (a thermally assisted Ostwald ripening with a most likely mass transport of small ZnO units along the particle surface) is emphasized.

(25) *Physik*; Rennert, P., Ed.; VEB Bibliographisches Institut Leipzig: Leipzig, 1986.

(26) Lifshitz, I. M.; Slyozov, V. V. *J. Phys. Chem. Solids* **1961**, *19*, 35.

(27) Wagner, C. *Z. Elektrochem.* **1961**, *65*, 581.

Further information about the structure of the nanometer-sized ZnO particles can be achieved from the thermal analysis. The mass loss according to the decomposition of adherent acetate was found to be 6.9 wt %. In the investigation of ZnO particles with a size of about 4.3 nm (as determined by the Scherrer method), Sakohara and co-workers found a loss of 25 wt % in the same temperature interval.<sup>28</sup> Additionally, they observed a loss of 5 wt % due to desorption of water and carbon dioxide at lower temperatures which has to be compared to the loss of 1.5 wt % in our study. Both values are about 3.5 times higher than the loss in our work. The particle size as determined from the TEM images in our examination was 5.6 nm. Assuming that the coverage of the surface with acetate for the samples used in both studies is virtually the same, the factor of 3.5 would lead to a particle diameter of 3.0 nm instead of 4.3 nm for the samples used by Sakohara and co-workers. This seems to be a more likely value for the actual size of the small nanocrystals.

According to the thermal analysis, the mass loss corresponding to the decomposition of acetate was 6.9 wt %. On the other hand, the absolute content of acetate as determined by elemental analysis for a ZnO sample dried in vacuo is calculated to be 10.9 wt % resulting in a difference of 4.0 wt %. For the latter examination, particles with a smaller diameter were chosen to enhance the surface area and the detection of adsorbed substances. Thus, the difference of 4.0 wt % may also arise from the different sizes.

Since the ZnO was thoroughly washed prior to the elemental analysis, it is unlikely that separate acetate crystallites were present in the sample. It is more probable that the acetate is strongly chemisorbed at the surface of the nanoparticles, acting as a complex ligand of surface Zn<sup>2+</sup> ions. Furthermore, the low molar ratio of C/H indicates that there are barely any OH groups at the surface of the sample dried in vacuo. This assumption is in agreement with the results of ESR spectroscopic investigations of the 2 nm sized starting colloid published by Micic and co-workers.<sup>29</sup> By examining an aqueous solution of the Spanhel–Anderson colloid upon laser irradiation, the authors found no indication for a charge transport from the semiconductor to surface OH groups. These findings may lead to the conclusion that the OH groups of the ZnO are either not accessible for a charge transfer or not even present in the colloidal solution.

The high lithium content as established by the elemental analysis is remarkable since there is no indication for a distortion of the ZnO crystal lattice by an incorporation of lithium ions. On the other hand, it was not possible to remove these ions simply by extensive washing (e.g., lithium acetate would have a high solubility in aqueous solvents). Hence, it must be expected that the Li<sup>+</sup> is not incorporated deep inside the ZnO lattice but is rather located in the few monolayers next to the surface of the particles. Additionally, no separate crystalline lithium compounds were found in the XRD patterns for all samples thus ruling out a

phase separation during the annealing process. Since lithium is a very light element, it cannot be readily seen in the TEM images. Thus, the as-prepared sample most likely consists of a core of pure ZnO, surrounded by a thin shell of lithium containing ZnO at the surface which is virtually not affected by the annealing process.

The absorption spectrum of an as-prepared ZnO thin film shows a blue shift of the absorption edge compared to the bulk semiconductor. This can be interpreted by an increase of the electronic band gap according to the size-quantization effect. Thus, the ZnO film has to consist of particles whose size must be of the same dimensions as the exciton in this material. As in most oxidic semiconductors, the Bohr radius of the exciton in ZnO is quite small (about 1 nm; however, it should be stated that the material constants required for the calculation of the Bohr radius are not properly known for the nanometer-sized materials). Thus, it is surprising that even the samples annealed at 400 °C with a diameter of about 10 nm still exhibit a blue shift of absorption. According to the literature, a quantization in ZnO colloids is known only for particle diameters up to 7 nm.<sup>6</sup> This contradiction might be explained by the assumption that the real volume accessible for the exciton is smaller than the actual geometric size of the crystallites. The XRD data as well as the TEM images gave no indication of the presence of different crystalline domains inside the particles. Hence, the additional spatial confinement might arise from the existence of a potential barrier at the surface which extends to the inner part of the ZnO particle. In a molecular picture, this barrier can be explained by different approaches: First, the existence of a lithium containing insulating layer at the surface could be responsible for the potential barrier as was concluded from the results of the thermal analysis. Moreover, an irregular stacking of the particles having no coherent superstructure might limit the space accessible to charge carriers. The latter can result in a distortion of the valence and the conduction band at the grain boundaries and thus in the formation of a potential barrier. Furthermore, the negatively charged acetate ions at the particle's surface may result in an electrostatic repulsion of the electrons inside the ZnO as was already assumed by Bahnemann and co-workers.<sup>14</sup> By the annealing of the films, the acetate is decomposed thus facilitating the electron transition between adjacent particles.

Additionally, the electrostatic interaction of the adsorbed acetate might result in a slight upward bending of the electronic bands of the ZnO particle toward its surface. Thus, the electronic levels inside the particle are energetically favored with respect to the levels at the surface. This might lead to a local increase of the electron density and hence a shift of the lowest electronic transition toward higher energies as is described by the theory of Burstein<sup>30</sup> and Moss.<sup>31</sup> A comparable shift has already been observed in spectroelectrochemical investigations of ZnO thin films by Hoyer and co-workers.<sup>19</sup> It should finally be mentioned that the consequences of such a repulsive force have also been seen in the fluorescence spectra of particulate ZnO

(28) Sakohara, S.; Tickenan, L. D.; Anderson, M. A. *J. Phys. Chem.* **1992**, *96*, 11086.

(29) Micic, O. I.; Zhang, Y.; Cromack, K. R.; Trifunac, A. D.; Thurnauer, M. C. *J. Phys. Chem.* **1993**, *97*, 7277.

(30) Burstein, E. *Phys. Rev.* **1954**, *93*, 632.

(31) Moss, T. S. *Proc. Phys. Soc., London* **1954**, *B67*, 775.

films and will be discussed in a forthcoming paper.<sup>32</sup>

All these effects might contribute to the observed spectral shift. Since the Coulomb interaction is a long-range interaction, the electrorepulsive approach is most likely able to explain the relation between the particle growth and the shift in the absorption spectra.

Besides the possibility of simply tailoring the band gap of ZnO via the stabilizing agent, this finding might be important for the improvement of existing designs of electrooptical devices since it might permit a better

charge transport through nanocrystalline oxidic structures.

**Acknowledgment.** We are gratefully indebted to Andreas Kornowski for the excellent TEM images. The authors also wish to thank Joachim Ludwig from the Mineralogisch-Petrographischen Institut who carried out the XRD measurements and Uta Sazama from the Institut für Anorganische und Angewandte Chemie who performed the thermal analysis.

---

(32) Noack, V.; Eychmüller, A. In preparation.